Construction and Building Materials 52 (2014) 488–493

Contents lists available at ScienceDirect

Construction and Building Materials

journal homepage: www.elsevier.com/locate/conbuildmat

# Influence of particle size on the early hydration of slag particle activated by $Ca(OH)_2$ solution

Zhijun Tan [a,*], Geert De Schutter [a], Guang Ye [a,b], Yun Gao [a], Lieven Machiels [c]

[a] Magnel Laboratory for Concrete Research, Department of Structural Engineering, Ghent University, Technologiepark-Zwijnaarde 904, B-9052 Ghent, Belgium
[b] Microlab, Faculty of Civil Engineering and Geosciences, Delft University of Technology, 2628 CN Delft, The Netherlands
[c] Centre for High Temperature Processes and Sustainable Materials Management, Department Metallurgy and Materials Engineering, KU Leuven, Kasteelpark Arenberg 44, B-3001 Leuven, Belgium

## HIGHLIGHTS

- Hydration and chemical compositions of slag were measured according to different size fractions.
- The calculation of hydration speed was conducted at particle level and based on measured particle size distribution.
- The hydration speed of slag particle is denoted as the rate of increase of the hydrating layer thickness.
- Higher $k$ value of slag particle arises from its chemical composition.

## ARTICLE INFO

*Article history:*
Received 2 October 2013
Accepted 20 November 2013

*Keywords:*
Blast-furnace slag
Particle size distribution
Reactivity
Hydration degree

## ABSTRACT

This paper investigates the influence of slag particle size on its hydration speed at particle level in the early age. Slags were separated with sieves into groups of different size fractions, considering a wide range of sizes. The chemical compositions of each group were analyzed by X-ray Fluorescence (XRF). Activated by 15% $Ca(OH)_2$ (by mass) at water/powder ratio 1:1, the hydration heat evolution was recorded by isothermal calorimetry up to 84 h and converted to hydration degree. Based on the hydration degrees and particle size distributions, the rate of increase of hydrating layer thickness of each single slag particle ($k$ value) was calculated. Results reveal that $k$ values of coarse particles are higher than that of fine particles. Coarse particles contain higher content of CaO but relatively lower content of MgO, $Al_2O_3$ and $SiO_2$, resulting in higher reactivity index of $(CaO + Al_2O_3 + MgO)/SiO_2$.



## 1. Introduction

Ground granulated blast-furnace slag (GGBFS) is widely used as construction material due to its latent cementitious property when mixing with lime, alkali-hydroxides or Portland cement. To improve the use of the slag in cement industry, a better understanding is needed of its hydration process. Modeling the hydration of cementitious materials improves this understanding [1]. It is of paramount importance to know the reactivity of slag when simulating the hydration process of slag. The reactivity of slag is usually estimated by the overall hydration rate or overall kinetics of slag hydration. Investigation [2] shows that the overall reactivity of slag is generally influenced by its glass content chemistry and particle size distribution (PSD). Additionally, process conditions also determine its reactivity, such as the process curing temperature, water/solids ratio and the ratio of slag to cement [3].

From the standpoint of overall kinetics, it is obvious that slag made up of fine particles reacts faster than that of coarser particles, since the former has significantly larger specific surface area than the latter. The hydration of a single slag particle takes place by moving the reaction front inwards, thus the rate of increase of the hydrating layer thickness of a single particle is worthwhile to know, which is applied as input by van Breugel [4] in HYMOSTRUC to simulate the hydration of Portland cement.

However, less attention has been paid to the influence of slag particle size on this parameter at particle level. Results of Sato et al. [5] and Chen et al. [6] showed that the thickness of the hydrating layer of a slag particle is not significantly influenced by its particle size. It should be noted that the particle sizes of the slag used in their experiments were in a narrow range, viz. from 3 to 13 μm, while the particle size of slag used in cement industry varies between micrometer and several hundred micrometers. Therefore, it is necessary to investigate the influence of slag particle size on its rate of increase of the hydrating layer thickness at a wider size range.

* Corresponding author. Tel.: +32 488471548.
*E-mail address:* zhijun.tan@ugent.be (Z. Tan).

0950-0618/$ - see front matter © 2013 Published by Elsevier Ltd.
http://dx.doi.org/10.1016/j.conbuildmat.2013.11.073

In this paper, two types of slag were separated into different size fractions by sieving. For each size fraction, the hydration process in the presence of $Ca(OH)_2$ solution was monitored up to 84 h by recording the heat evolution using the isothermal calorimetry method. The measured heat evolution of slag was further used to estimate the overall hydration degree. Based on the measured PSD and the assumed spherical shape of the slag particle, the hydration speed of slag particles was calculated for each size fraction, which is denoted as the rate of increase of the hydrating layer thickness of a single particle. Moreover, the chemical compositions and crystalline phase of each slag size fraction were analyzed using X-ray fluorescence (XRF) and quantitative analysis of the crystalline and amorphous phases performed by X-ray powder diffraction analysis (XRPD) with application of the Rietveld method, respectively.

## 2. Materials and methods

### 2.1. Materials and experiments

Two ground granulated blast-furnace slags were studied in this investigation, the first slag (slag 1) was offered by ORCEM company (the Netherlands) while the second (slag 2) was from Belgium origin. According to the fineness, slag 1 was sieved into 3 groups, viz. particle sizes (diameter) smaller than 20 μm, larger than 20 μm, and the original material (non-sieved). Slag 2 was sieved into 4 groups, viz. particle sizes smaller than 20 μm, larger than 20 μm but smaller than 40 μm, particle sizes larger than 40 μm, and original material. The PSD of the 7 groups of slag was measured using the laser diffraction method (Mastersizer 2000). Results are plotted in Figs. 1 and 2. The chemical compositions were analyzed by XRF. For XRF analysis the samples were pressed into powder tablets then the measurements were performed with a Panalytical Axios$^{mAX}$ WDXRF spectrometer. Data evaluation was processed with SuperQ5.0i/Omnian software. The results are indicated in Table 1. The mineralogy of the slags was determined by quantitative X-ray powder diffraction analysis (QXRPD, Philips PW1830). For the QXRPD preparation, 10 wt.% of analytical grade crystalline ZnO was added and the slag-standard mixture was milled (McCrone Micronizing mill) in ethanol for 7.5–10 min. Diffraction patterns were measured in $2\theta$ range of 10–70° using Cu Kα radiation of 45 kV and 30 mA, with a 0.02° step size and step time of 2 s. Quantitative results were obtained adopting the Rietveld method [7,8], using the "Topas® Academic" software [9]. A fundamental parameter approach was used, meaning that instrumental contributions to the peak shapes were calculated directly [10] and the standard parameters (cell parameters, crystallite size, lattice strain, diffraction optical effects and background) were refined. Results are given in Table 2. According to [11], reactivity moduli and Ca/Si molar ratios were calculated based on the obtained chemical compositions as shown in Table 3.

For the isothermal calorimetry test, 8.5 g slag taken from each group was mixed in an ampoule with 1.5 g $Ca(OH)_2$ powder and 10 g deionized water. The well mixed paste was immediately placed in a TAM AIR isothermal heat conduction calorimeter (TA instrument) at a temperature of 20 °C. The evolution of hydration heat was recorded every minute up to 84 h, and each heat release curve was obtained by averaging three replicate samples. In this paper, the ratio of cumulative heat evolution of the slag to its theoretical maximum value is considered as overall hydration degree. The theoretical maximum heat release of slag is taken as 461 J/g [12].

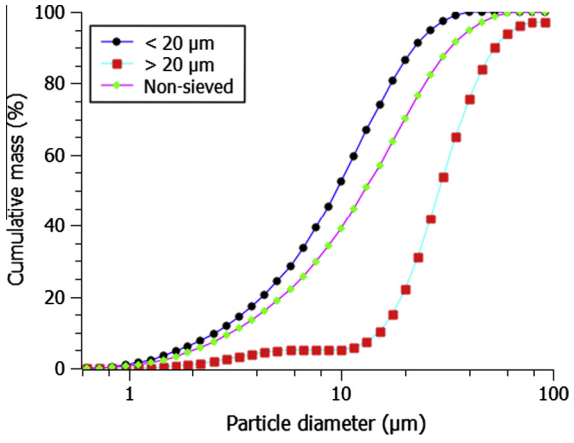


**Fig. 1.** Particles size distribution of slag 1, fraction < 20 μm: 91.3%, fraction > 20 μm: 84.9%.

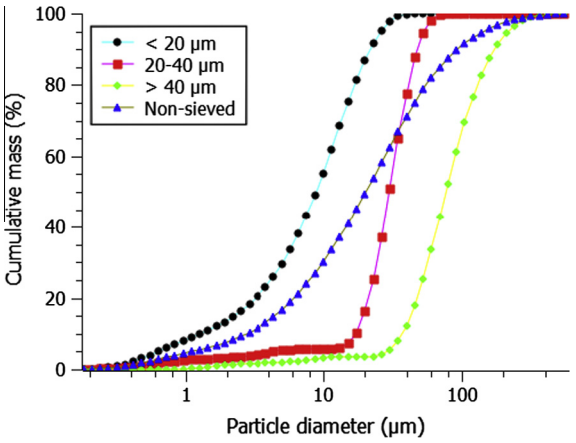


**Fig. 2.** Particles size distribution of slag 2, fraction < 20 μm: 91.60%, fraction 20–40 μm: 77.3%, fraction > 40 μm: 91.9%.

### 2.2. Calculation method

Fig. 3 shows a schematic representation of a hydrating slag particle. The parameter $k$ denotes the average rate of increase of the hydrating layer thickness for a single slag particle (the unit of $k$ in this paper is μm/day). The $k$ value of a single particle is calculated by linking the overall hydration degree with the thickness of the hydrated layer of the particles. The establishment of this link is based on four assumptions as proposed below.

- The shape of slag particles is assumed as spherical (Fig. 3) to facilitate the calculation at particle level. The diameters and size fractions were measured by laser diffraction method.
- The first hydration stage is assumed as phase boundary reaction [13], thus the thickness of the hydrated layer of a slag particle increases with time following a first order relation (Fig. 3 and Eq. (1)):

$$k = \delta_{in(t)}/t \tag{1}$$

where $\delta_{in(t)}$ is the thickness of the hydrating layer of a slag particle at reaction time $t$. It has to be noted that in this paper $k$ is assumed as an average value of a particle from the start of hydration to the calculation time $t$ and all slag particles in the same group have the same $k$ value. The simplification here is for the sake of practical computer calculation.

- Since there is sufficient space for the expanding volume of each hydrating slag particle, it is assumed that there is no interaction between particles in the hydrating system. This simplification is far away from the reality at regular water to paste ratios, e.g. 0.5, but it is reasonable in this paper because the water to paste ratio used is 1:1.
- Due to sufficient quantity of water and $Ca(OH)_2$ for the hydration of slag, the hydration speed of slag particles in the paste is assumed to be not limited by the shortage of reactant.

Based on the above assumptions, the calculation of $k$ is carried out as follows. For each group of slag, 1 g of slag particles is taken as the calculation target. The hydration degree $\alpha_{(r,t)}$ of a single particle is calculated based upon the thickness of the hydrated slag layer, $\delta_{in(t)} = k\,t$, then

$$\alpha_{t,r} = 1 - (1 - \delta_{in(t)}/r)^3 \tag{2}$$

where $r$ is the radius of the slag particle that is obtained from the PSD result. The hydration degree ($\alpha_{(total,\ t,\ r)}$) of all slag particles with the same size $r$ in 1 g of slag is also $\alpha_{(t,\ r)}$.

The total hydration degree $\alpha_{(total,\ t)}$ of the entire 1 g of slag from the beginning of hydration to time $t$ is obtained:

$$\alpha_{total,t} = \sum_{r=r_{min}}^{r_{max}} f_r * \alpha_{total,t,r} \tag{3}$$

where $f_r$ obtained from PSD tests is the mass fraction of particles with the same size $r$, which is determined by laser diffraction method. The parameters $r_{max}$ and $r_{min}$ are obtained from PSD analysis and are the maximum and the minimum radius of particles respectively.

**Table 1**
The chemical compositions of slag tested by XRF (mass%).

| Name | Slag 1 | | | Slag 2 | | | | Error (%) |
|---|---|---|---|---|---|---|---|---|
| | <20 μm | >20 μm | Non-sieved | <20 μm | 20–40 μm | >40 μm | Non-sieved | |
| CaO | 38.18 | 39.61 | 38.14 | 39.42 | 41.57 | 42.09 | 40.01 | 0.10 |
| $SiO_2$ | 35.87 | 34.64 | 35.82 | 36.14 | 34.72 | 34.23 | 35.75 | 0.10 |
| $Al_2O_3$ | 12.07 | 11.75 | 12.05 | 10.98 | 10.52 | 10.32 | 10.70 | 0.09 |
| MgO | 9.33 | 9.24 | 9.37 | 10.08 | 9.64 | 9.64 | 9.99 | 0.09 |
| $SO_3$ | 1.75 | 1.70 | 1.76 | 1.39 | 1.37 | 1.34 | 1.39 | 0.04 |
| $TiO_2$ | 0.97 | 1.10 | 1.05 | 0.57 | 0.67 | 0.66 | 0.61 | 0.02 |
| $K_2O$ | 0.48 | 0.48 | 0.48 | 0.37 | 0.37 | 0.38 | 0.36 | 0.02 |
| $Fe_2O_3$ | 0.42 | 0.50 | 0.41 | 0.27 | 0.28 | 0.40 | 0.28 | 0.02 |
| MnO | 0.45 | 0.53 | 0.45 | 0.26 | 0.31 | 0.34 | 0.31 | 0.02 |
| $Na_2O$ | 0.17 | 0.16 | 0.16 | 0.21 | 0.18 | 0.19 | 0.23 | 0.01 |

**Table 2**
Main crystalline phases of slag tested by XRD/Rietveld (mass%).

| Name | Slag 1 | | | Slag 2 | | | |
|---|---|---|---|---|---|---|---|
| | <20 μm | >20 μm | Non-sieved | <20 μm | 20–40 μm | >40 μm | Non-sieved |
| Akermanite | 0.7 | 0.8 | 0.9 | / | / | / | / |
| Calcite | / | / | / | 2.2 | 1.1 | 0.4 | 0.5 |
| $C_2S$ | / | / | / | 3.4 | 3.0 | 3.5 | 4.1 |
| $C_4AF$ | / | / | / | 1.9 | 1.2 | 0.4 | 1.0 |
| $C_3A$ | / | / | / | 0.7 | 1.2 | 1.4 | 1.0 |
| Quartz | 0.5 | 0.8 | 1.3 | 2.7 | 2.0 | 1.7 | 1.2 |
| Total crystalline content | 1.6 | 1.3 | 2.2 | 12.7 | 10.4 | 9.7 | 8.7 |

**Table 3**
Reactivity moduli and Ca/Si of slag.

| Name | Slag 1 | | | Slag 2 | | | |
|---|---|---|---|---|---|---|---|
| | <20 μm | >20 μm | Non-sieved | <20 μm | 20–40 μm | >40 μm | Non-sieved |
| (C + A + M)/S | 1.66 | 1.75 | 1.66 | 1.67 | 1.78 | 1.81 | 1.70 |
| (C + M)/S | 1.32 | 1.41 | 1.33 | 1.37 | 1.48 | 1.51 | 1.40 |
| A/S | 0.34 | 0.34 | 0.34 | 0.30 | 0.30 | 0.30 | 0.30 |
| (C + M)/(S + A) | 0.99 | 1.05 | 0.99 | 1.05 | 1.13 | 1.16 | 1.08 |
| Ca/Si | 1.14 | 1.23 | 1.14 | 1.17 | 1.28 | 1.32 | 1.20 |

C = CaO, A = $Al_2O_3$, S = $SiO_2$, M = MgO.

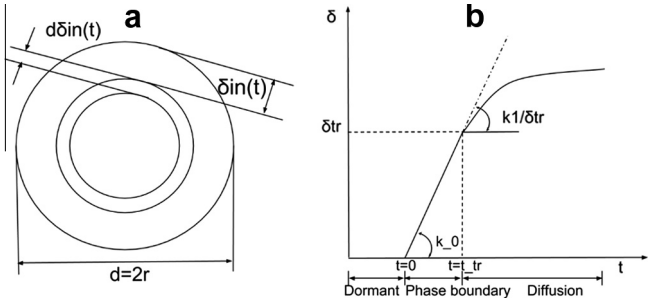


**Fig. 3.** Schematic representation of a hydrating slag particle: (a) the thickness of the hydrating layer and (b) $k$ is a constant in the phase boundary stage; the kinetics follows a first order relation [4].

Equaling the numerically calculated $\alpha_{(total,\ t)}$ and the experimentally recorded total hydration degree $\alpha_{(total,t,e)}$, the value $k$ can be numerically calculated. For all cases, knowing the experimentally obtained PSD and the overall hydration degree, we can calculate the average rate of increase of the hydrating layer thickness of slag particles for each group, viz. $k$ value.

## 3. Results

### 3.1. Heat evolution rate and cumulative heat

Figs. 4 and 5 display the heat evolution rate of each group of slag. The first peak occurs in the first minutes, and may arise from the physical wetting instead of chemical reaction [14]. A second peak of heat evolution rate appears after about 10–20 h. The maximum value of the second rate peak is much lower than the first one, but the cumulative heat evolution is more important as the second peak spreads over a longer time period. Peak values of finer slag particles are as high as 5 times that of the coarse particles, e.g. the second peak of heat evolution rate of slag particles larger than

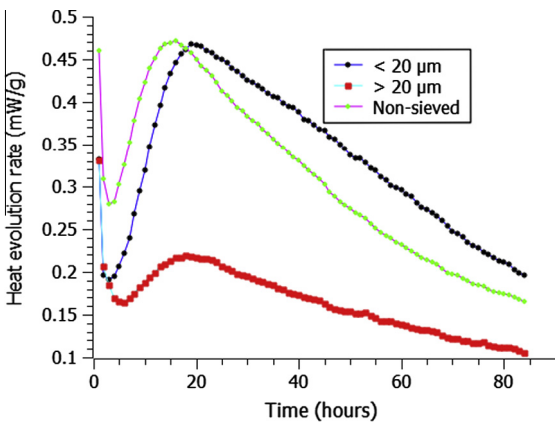


**Fig. 4.** Heat evolution rate of slag 1.

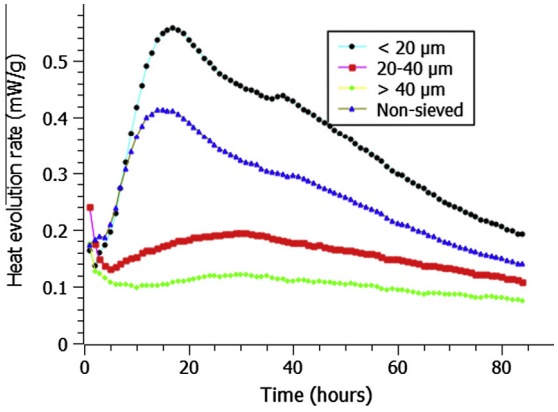


**Fig. 5.** Heat evolution rate of slag 2.

40 μm (Fig. 5) is only 0.12 mW/g when the reaction proceeded 25 h, while that of the particles smaller than 20 μm is 0.56 mW/g occurring after 17 h hydration.

Figs. 6 and 7 show the cumulative heat evolution of the slag. After the first half hour that corresponds to the wetting peak, the cumulative heat evolution steadily increases. Coarse particle groups release less heat than fine groups, which is even more distinct at the later stage. It is easy to understand the difference of cumulative heat evolution. Since a group of fine slag has significantly larger specific surface area than that of a coarse group, e.g. specific surface area (or surface area per mass unit) of spherical particles with diameter 1 μm is 10 times that of particles with diameter 10 μm.

### 3.2. Calculated k values

Based on the aforementioned four assumptions and the calculation method, the rate of increase $k$ of hydrating layer thickness of the slag particles in each group of slag was calculated. The calculated results of $k$ corresponding to each hydration time period $t$ are plotted in Figs. 8 and 9.

As can be seen from the results, the $k$ of the coarse slag fraction is always higher than of the fine group, which means that the rate of increase of the hydrating layer thickness of a single slag particle from a coarse group is faster than that from a fine group. Additionally, the $k$ value sharply decreases from high to low values in the first 20 h of hydration and then steadily reaches relatively stable values, which also confirms the aforementioned assumptions that

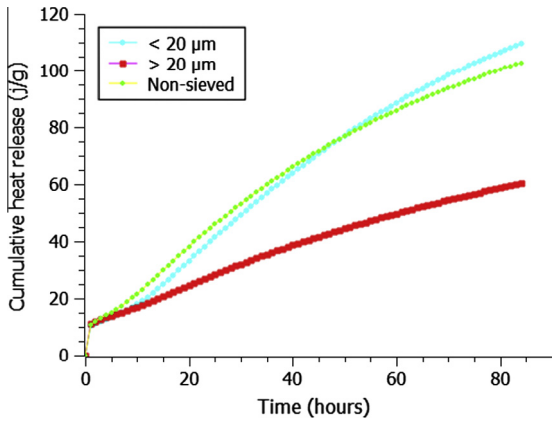


**Fig. 6.** Cumulative heat release of slag 1.

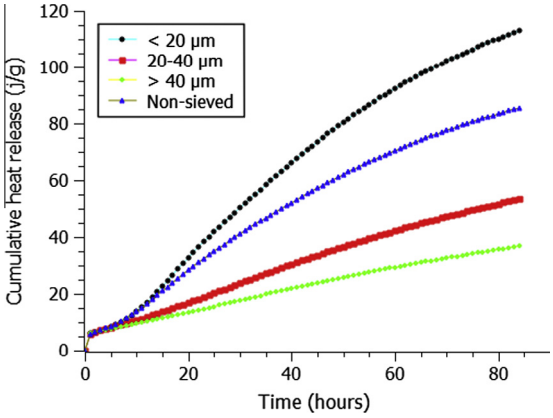


**Fig. 7.** Cumulative heat release of slag 2.

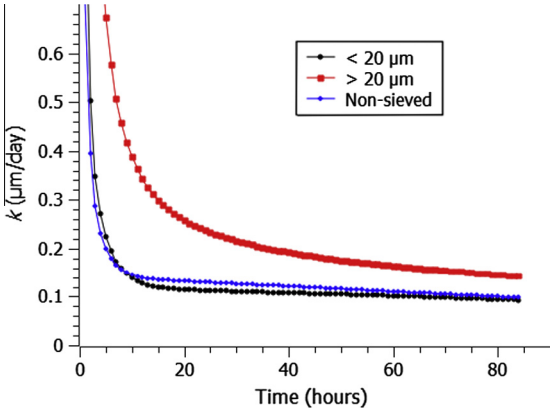


**Fig. 8.** Calculated $k$ values of slag 1.

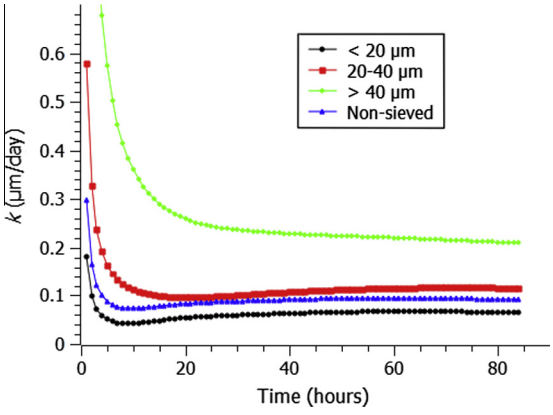


**Fig. 9.** Calculated $k$ values of slag 2.

the thickness of the hydrated layer increases with time following a first order relation.

Table 4 and 5 summarize the calculated $k$ value of each group of slag after 72 h of hydration. Among these values, the lowest $k$ value is 0.066 μm/d, of particles smaller than 20 μm from slag 2, while the highest is 0.216 μm/d of particles larger than 40 μm from slag 2. Corresponding values of Portland cement particles range from 0.6 to 1.32 μm/d [4]. Compared to Portland cement particles, the lower $k$ of slag particles explains the slow hydration process of slag. According to [15] slag particles can gradually react until the thickness of the reaction layer reaches about 0.3–0.5 μm. The

**Table 4**
Calculated $k$ of slag 1 after 72 h hydration (μm/d).

| Non-sieved | <20 μm | >20 μm |
|---|---|---|
| 0.104 | 0.098 | 0.153 |

**Table 5**
Calculated $k$ of slag 2 after 72 h hydration (μm/d).

| Non-sieved | <20 μm | 20–40 μm | >40 μm |
|---|---|---|---|
| 0.094 | 0.066 | 0.116 | 0.216 |

reaction rate may be subsequently hindered by the texture of the hydration products. This implies that the hydration of slag in this investigation switches from phase boundary to diffusion controlled hydration after about 72 h of hydration when the hydrated thickness is already 0.3 μm. At higher age, the kinetics function for the first stage, i.e. Eq. (1), in principle can no longer be applied to calculate $k$.

## 4. Discussion

### 4.1. Extended discussion on simplification of calculation

The experimental method is of paramount importance to investigate the hydration kinetics of slag. Compared with EDTA method [3], isothermal calorimetry is a continuous way to record the hydration process especially in the early age. The high accuracy of TAM AIR guarantees reliable results of the heat evolution rate during the hydration process.

The maximum heat release of the final hydration of slag is taken as 461 J/g, based on limited literature data. This value is questionable, but unfortunately there is no formula to calculate the maximum heat of slag hydration, while a large body of data can be used to calculate the maximum heat of hydration of Portland cement. The maximum heat evolution of complete slag hydration is supposed to be a function of chemical composition and its vitreous fraction. Since the maximum heat evolution of slag hydration is not the topic of this paper, the value 461 J/g is simply applied to convert the heat evolution to hydration degree.

The shape of slag is assumed as spherical in this paper to simplify the numerical calculation of rate of increase of hydrating layer thickness of slag particle. In this way, only having the diameter of the particle is sufficient for the given mathematical expressions. The diameter of the particles is measured using laser diffraction method. However, the spherical shape of slag particles is definitely not realistic. Extensive analysis [16] of geometric characteristics of slag particles using SEM shows that the real shape of slag particles is irregular. It should be born in mind that the assumption of spherical shape underestimates the specific surface area of slag particles.

As seen from the PSD results, the sieving process adequately separated the slag particles by different sizes. Due to the irregular shape of slag, some overlap exists to a marginal extent, e.g., a small amount of particles smaller than 20 μm cannot be separated into the group smaller than 20 μm, while some particles larger than 20 μm go through the 20 μm sieve, to stay in the group smaller than 20 μm as well. This phenomenon also occurs in the case of sieving at 40 μm, as shown by the PSD results in Figs. 1 and 2. To account for the overlapping of sizes, the measured PSD of each group is applied in the calculation. Since the amount of these overlapped sizes is only a few percentages, its influence is not significant for the calculation of $k$.

The calculation of $k$ does not consider possible interaction among particles and the influence of varying ion concentration of the pore solution in the paste. This simplification is based on the high water/solid ratio (1:1), because the large amount of water guarantees enough space for the precipitation of hydration products and a relatively stable ion concentration in the solution.

### 4.2. Influence of particle size on hydration speed of slag particle

Based on the measured hydration process of slag with different sizes, the calculated results demonstrate that the rate of increase of the hydrating layer thickness of coarse slag particles is faster than that of fine particles.

The chemical composition analysis of slag by XRF reveals a difference among the 7 slag groups of different sizes. As the slag size increases, the CaO content slightly increases, while the contents of other oxides such as MgO, $Al_2O_3$ and $SiO_2$ decrease. Although the changes are rather small, there is a substantial change in in the (C + A + M)/S ratio and thusthe reactivity index of slag [17]. The reactivity indices calculated from the XRF results suggest that the coarser slag fraction has higher reactivity, e.g. according to the German standard, the calculated reactivity index (C + A + M)/S (Table 3) of the coarser particle group is higher than of the fine group, which coincides with the faster rate of increase of hydrating layer thickness, i.e. higher $k$ value.

Taylor mentioned [18] that small contents of crystalline phases in slag can provide nucleation sites for hydration products, and can thus accelerate the hydration process. The content of crystalline phase of the two types of slag varies significantly, but there is not too much difference in terms of $k$ values of the two non-sieved groups. The content of crystalline phase of each group from the same slag varies as size changes. However, considering the accuracy of XRD/Rietveld and the relatively low content of crystalline phase in this study, we do not believe that the $k$ value is significantly influenced by the crystalline phase.

The influence of particle size on hydration speed of slag particle investigated in this paper is essentially attributed to the chemical composition. Slag particles of different sizes are formed by the grinding process. A possible reason accounting for the different sizes is owing to the different hardness of slag particles, and the hardness may be determined by the intrinsic chemical compositions, e.g. higher CaO content may leads to higher hardness of slag in this paper, which needs to be further investigated.

Research indicated that amorphous silicate and aluminate phases are the main cementitious phases in slag and mainly exist in the small particles [19]. XRF results of this investigation also confirm that slag groups of small sizes contain higher content of $Al_2O_3$ and $SiO_2$ than the corresponding values of slag groups consisting of large particles.

However, another important property of slag is alkalinity. To assess the activity of steel slag, Mason [20] proposed a method to calculate the alkalinity (denoted as M), which is defined as $M = w(CaO)/[w(SiO_2) + w(P_2O_5)]$. Tang et al. [21] also indicated that the major mineral compositions of steel slag depend on its alkalinity. It might be doubtful to directly apply the knowledge from steel slag to GGBFS, but higher Ca/Si ratio of GGBFS with larger size in this study could account for the faster rate of increase of the hydrating layer thickness, i.e. $k$ value.

It is known that the Ca–O and Mg–O bonds are weaker than Al–O and Si–O in the glassy slag surface under the polarization effect of $OH^-$ [22], which implies that it is easier to break the surface of slag particle with more CaO but less $SiO_2$. Therefore, coarse slag particles with higher content of CaO are more vulnerable to the attack of $OH^-$, leading to higher $k$ value in this study.

Further literature indicates that the reaction kinetics of slag particles can be influenced by the Ca/Si ratio of hydration products.

On the one hand, according to the research from Glasser [23], as the Ca/Si ratio declines to less than 1.2–1.3, the electric surface charge of C–S–H gel gradually reverses from positive to negative. The less positive or even negative charges on the surface of C–S–H gel attract $Ca^{2+}$ ions of pore solution moving towards inner hydration products and then reacting with silicate ions, which results in denser inner product having stronger resistance against further ion diffusion. On the other hand, C–S–H gel with a lower Ca/Si ratio has a foil-like morphology rather than fibrillar one, implying the tortuosity of gel pores becomes higher and the path for ion diffusion is elongated. In all, the changed surface charges and morphology of C–S–H gel with lower Ca/Si ratio hamper the reaction front developing inwards.

Since the Si and Ca ion concentrations in pore solution are considerably low (<20 mmol/L), the Ca/Si ratio of C–S–H gel is mainly determined by that of slag material. The Ca/Si ratio of slag in this study ranges from 1.14 to 1.32 as listed in Table 3. The Ca/Si ratio of fine slag group is lower than that of coarse group due to its lower content of CaO and higher $SiO_2$. The lower Ca/Si ratio of small slag particle results in lower Ca/Si of C–S–H gel that leads to less positive surface charges and foil-like morphology, which accounts for the slower rate of increase of the hydrating layer thickness (i.e. lower $k$ value).

Based on the aforementioned elements, it can be concluded that the Ca/Si of slag is crucial for the reactivity of slag particles at least in the early age of hydration. A coarse slag particle has a higher Ca/Si ratio, which in turn brings a higher rate of increase of the hydrating layer thickness.

Though the rate of increase of the hydrating layer thickness ($k$ value) of fine slag particles is slower than that of coarse particles, increasing fineness of slag is still of paramount importance to boost the overall reactivity of hydration. The reason is that $k$ values of fine slag particles and coarse particles are of the same order of magnitude, while the specific surface area of the former is one order of magnitude higher than that of the latter. Meanwhile, coarse slag particles (e.g. diameter larger than 40 μm) usually make up a relatively small part in slag. The combined effect of particle size and surface area on overall hydration is confirmed by the experiment results that the cumulative heat evolution of the fine slag fraction is higher than the coarse fraction after the same hydration time. This may explain why less attention has been paid to the influence of particle size on the hydration speed of slag at particle level.

## 5. Conclusions

The influence of particle size on the hydration speed of slag at particle level activated by $Ca(OH)_2$ was investigated in this study, that the following conclusions have been obtained:

- The overall hydration degree of slag consisting of fine particles develops faster than that of coarse slag due to its large specific surface area.
- Slag made up of coarse particles has higher content of CaO but relatively lower content of MgO, $Al_2O_3$ and $SiO_2$, resulting in higher reactivity index of $(CaO + Al_2O_3 + MgO)/SiO_2$, which implies higher reactivity at particle level.
- Particle size of slag has influence on the rate of increase of the hydrating layer thickness of a single slag particle ($k$ value). The $k$ values of coarse particles are higher than that of fine particles.
- The influence of particle size on the hydration of slag is essentially attributed to the chemical compositions. Higher Ca/Si ratio of slag is crucial for the reactivity of slag particles at least in the early stage of hydration.

## Acknowledgement

The authors gratefully acknowledge the financial support from the special research fund (BOF) of Ghent University.

## References

[1] van Breugel K. Modelling of cement-based systems – the alchemy of cement chemistry. Cem Concr Res 2004;34:1661–8.
[2] Escalantea JI, Gómeza LY, Johalb KK, Mendozaa G, Manchaa H, Mendez J. Reactivity of blast-furnace slag in Portland cement blends hydrated under different conditions. Cem Concr Res 2001;31:1403–9.
[3] Lumley JS, Gollop RS, Moir GK, Taylor HFW. Degrees of reaction of the slag in some blends with Portland cements. Cem Concr Res 1996;26:139–51.
[4] K. van Breugel. Simulation of hydration and formation of structure in hardening cement-based materials. Doctoral Thesis. Delft University of Technology, The Netherlands; 1997. p. 109, p. 166–168.
[5] Sato K, Konish E, Fukaya K. Hydration of blast-furnace slag particle. In: Proc. 8th ICCC, vol. 4. Brazil: Rio de Janeiro; 1986. p. 98–03.
[6] Chen Wei, Brouwers HJH, Shui ZH. Three-dimensional computer modeling of slag cement hydration. J Mater Sci 2007;42:9595–610.
[7] Rietveld HM. A method for including the line profiles of neutron powder diffraction peaks in the determination of crystal structures. Acta Crystallogr 1966;21:A228.
[8] Rietveld HM. A profile refinement method for nuclear and magnetic structures. J Appl Crystallogr 1969;2:65–71.
[9] Coelho AA. TOPAS-Academic: A Computer Programme for Rietveld Analysis, 2004. http://www.topas-academic.net.
[10] Cheary RW, Coelho AA. A fundamental parameters approach of X-ray line-profile fitting. J Appl Crystallogr 1992;25:109–21.
[11] Kocaba V. Development and evaluation of methods to follow microstructural development of cementitious systems including slags. Doctoral Thesis. École Polytechnique Fédérale de Lausanne, Suisse; 2009. p. 48.
[12] Kishi T, Maekawa K. Thermal and mechanical modeling of young concrete based on hydration process of multi-component cement minerals. In: Springenschmid R, editor. Proceedings of the international RILEM symposium on thermal cracking in concrete at early ages London: E&FN Spon; 1995. p. 11–18.
[13] Ye G, van Breugel K. Microstructure simulation of Portland cement blended with blast furnace slag. In: International RILEM symposium on concrete modeling, Delft, the Netherlands, 2008. p. 791–00.
[14] Shi Caijun. Robert l. Day. A calorimetric study of early hydration of alkali-slag cements. Cement and Connete Research. Cem Concr Res 1995;25:1333–46.
[15] Otsuka Y, Ueki Y, Dan Y, Goto S. Effects of the fineness of blast furnace slag on the hydration of high-sulfated slag cement. In: Proc. 13th ICCC, Madrid, Spain, 2011.
[16] Wan Huiwen, Shui Zhonghe, Lin Zongshou. Analysis of geometric characteristics of GGBS particles and their influences on cement properties. Cem Concr Res 2004;34:133–7.
[17] Scrivener KarenL, Nonat Andre. Hydration of cementitious materilas, present and future. Cem Con Res 2011;41:651–65.
[18] Taylor HFW. Cement chemistry. London: Thomas Telford; 1997. p. 264.
[19] Wang Qiang, Yana Peiyu, Feng Jianwen. A discussion on improving hydration activity of steel slag by altering its mineral compositions. J Hazard Mater 2011;186:1070–5.
[20] Mason B. The constitution of some open-hearth slag. J Iron Steel Inst 1994;11:69–80.
[21] Tang MS, Yuan MQ, Han SF, Shen X. The crystalline state of MgO, FeO and MnO in steel slag and the soundness of steel slag cement. J Chin Ceram Soc 1979;7:35–46 [in Chinese].
[22] Shi Caijun, Day Robert L. A calorimetric study of early hydration of Alkali-slag cements. Cem Concr Res 1995;25:1333–46.
[23] Glasser FP. Chemistry of alkali-aggregate reaction. In: Swamy R, editor. The alkali-silica reaction in concrete. New York: Van Nostrand Reinhold; 1992. p. 30–53.